Rigorous Analysis of Multiple Coupled Rib Waveguides

Tullio Rozzi, *Fellow, IEEE,* M. N. Husain, and Leonardo Zappelli

Abstract—**The general problem of multiple coupled rib waveguides, where energy may be leaked from one guide to the other via the substrate and radiation mode, is of great practical and theoretical importance. Rigorous results including substrate and air modes coupling are hard to find for the general case of coupling of two or more different guides, due to the considerable complexity arising. In this contribution, we develop the analysis in terms of a cascade of the transverse steps, utilizing a variational solution with a single trial function and making explicit use of edge singularities at the dielectric corners in order to produce an effective and rigorous solution. Multiple coupled rib guides are then reduced to a cascade of interacting step discontinuities in the transverse direction. Where comparison is possible the numerical results obtained by the method are seen to be as accurate as those obtained by the FEM/FDM methods, but with a fraction of the computer time and memory involved.**

I. Introduction

COUPLED structures play a very important role in the field of millimeter waves and integrated optics. Arrays of coupled dielectric antennas are interesting for millimetric applications and laser arrays may be realized using coupled rib guides. The feasibility of fabricating such devices using coupled guides has been demonstrated and the near field and propagation characteristics of such arrays are already of great practical importance in integrated optics. As a consequence, accurate theoretical analyses of coupled structures are essential to the design of devices that meet specific requirements and criteria.

Coupled rib guides in a parallel plate configuration have been studied in [1] by transverse mode matching. There are no truly exact analytical method available for the analysis of multiple coupled rib waveguides in the open configuration. Approximate methods currently in use have mostly relied on either the EDC method [2]–[4], or coupled mode theory which is appropriate for weakly coupled systems [5]. The approach in [5] assumes the individual guided modes to be orthogonal in the coupled structure. An improved coupled mode theory [6], [7] which removes the assumption is also available. However, the EDC and the coupled mode theory fail to model the effects arising from leakage of energy via the substrate and the air regions, particularly, in the millimetric case. This effects may also be significant at optical frequencies, particularly if the rib height is large, where the interaction effects via the continuum cannot be neglected. For more accurate results, sophisticated numerical techniques such as Finite Element Method or Finite Difference Method are used [8]. The most important drawbacks of this approach, is the excessive computational effort needed for accurate results, as the area and hence the number of mesh points is doubled with respect to that needed to analyse a single guide. Moreover, FEM/FDM become extremely cumbersome for situations more complex than that of two identical closely coupled guides, as shown for instance in Fig. 1. This is the typical problem we are addressing in this contribution. We are considering pure LSE and LSM polarizations but extension to the hybrid case is straightforward though more cumbersome. The approach adopted in this work is consistent with that used in [9] for the single guide. The analysis is followed by application to the case of the directional coupler, three guide coupler, closely spaced unequal guide and wave guide arrays. Wherever possible, results of the present method and of the FEM/FDM analysis are compared to demonstrate the effectiveness and the accuracy of the method. As will be shown, the method of analysis presented in this work yields accurate results with a computational effort only slightly greater than that needed to analyse a single guide according to [9].

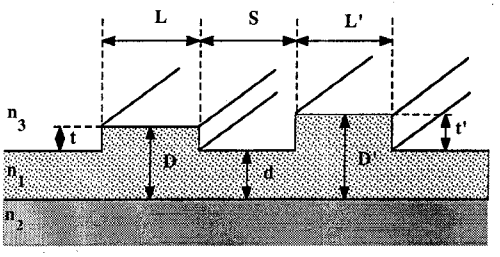

Fig. 1. Geometry of the coupled rib waveguides.

II. Theoretical Approach

The cross sectional geometry of coupled rib waveguides under consideration is shown in Fig. 1. In the framework of Transverse Resonance Diffraction (TRD), this configuration is seen as that of four cascaded step discontinuities in the transverse direction. Our aim is to

Manuscript received March 11, 1991; revised October 24, 1991.

T. Rozzi and L. Zappelli are with the Dipartimento di Elettronica ed Automatica, Università degli Studi di Ancona, 60131 Ancona, Italy.

M. N. Husain is with the School of Electrical Engineering, University of Bath, Bath, U.K.

IEEE Log Number 9106057.

derive a variational solution of the step problems that utilizes a single test function, the "transition function" developed in [9] in order to expand the unknown interface field. Using a single test function at the interface yields a simple two port equivalent network representation of the coupled structure such as shown in Fig. 2. Consequently, the analysis of the transverse cascade reduces to that of solving the two port network, which is easily effected by standard network technique. In order to derive the variational expression for the parameters of the two port network shown in Fig. 2, let consider the cross sectional geometry of Fig. 3 which represents the basic building component of the coupled structure in Fig. 1. In this case, the analysis is complicated by the presence of the two step discontinuities at $x = 0$ and $x = L$ (see Fig. 3). Considering the transverse propagation of LSE and LSM modes in such a structure, at each step discontinuity, continuous modes are excited and multiple reflections of these modes occur between the two steps. In applying standard transverse resonance to this situation, interaction via the continuous modes is ignored, i.e., a small step approximation is assumed. If this is done, then the uniform region and the step discontinuity can be represented by a transmission line and ideal transformer, respectively. Interaction via the continuum between the steps at $x = 0$ and $x = L$ of Fig. 3, however, is not representable by means of a finite number of transmission lines coupled at the discontinuities, as in a closed waveguide.

Hence, we abandon the transmission line analogy and adopt instead a two-port, "Tee" representation of each region between two successive steps. Its open-circuit impedance, short-circuit admittance parameters are obtained by placing a magnetic/electric wall at $x = 0, L$ in turn. Under "open circuit" and "short circuit" conditions at $x = 0, L$, integral operators are found relating the total E and H fields at various ports and then these are used to relate the total fields at each port to one another. This operator method was introduced in [10] in the treatment of cascaded longitudinal step discontinuities in slab waveguides. In that approach the field at each interface was developed in terms of a suitable set of expanding functions, a variational expression was derived and multiport analysis was finally used to model the cascade. Although those concepts seem directly applicable to the present problem, numerical effectiveness in solving a transverse resonance equation would be limited by the size of the network matrix, containing integrals over the continuum in each element. Moreover, the interface fields in the longitudinal step discontinuities are complex and consequently a complex trial field is needed to accurately expand them. Hence, a solution based on Galerkin's method is more appropriate to that situation. By contrast, in the present case, losslessness of the bound mode requires the interface fields at the transverse step discontinuities to be real. This suggests that the interface field be represented by a suitable real function. In this work, the interface field is approximated by a single "transition function," inclusive of the edge conditions in the LSM case as in [9]. As

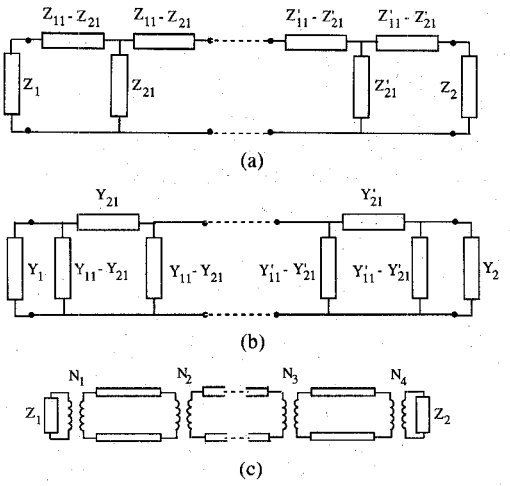

Fig. 2. Equivalent network representation of the coupled structure: (a) LSE case; (b) LSM case; (c) Neglecting interaction via continuous modes.

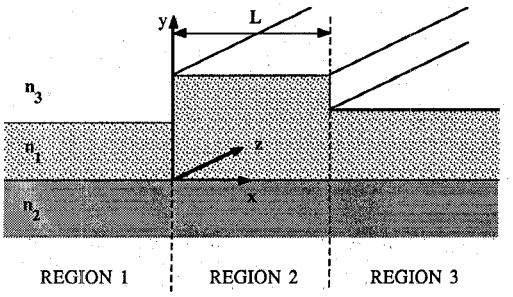

Fig. 3. Unit cell of the coupled structure showing double step discontinuity in the transverse x-direction.

a consequence the numerical complexity of the problem is substantially reduced, avoiding the use of matrices altogether. Furthermore, this formulation leads to an equivalent network model of the structure represented by a cascade of "T" or "π" two port networks as shown in Fig. 2.

LSE Analysis

Consider the situation where slabs 1 and 3 of Fig. 3 are semi-infinite. The relationship between the transverse electric E (z-directed) and the transverse magnetic field H (y-directed) at $x = 0^-$ is given by [9],

$$E(0, y) = -\int_{-\infty}^{\infty} Z_1(y, y')\,[-H(0, y')]\,dy' \equiv -\hat{Z}_1[-H(0, y')] \tag{1}$$

where

$$Z_1(y, y') = -\Big[z_{01}\psi_{h1}(y)\psi_{h1}(y') + \sum_{\mu=e,o}\int_0^{\infty} z_{01}(\rho)\psi_{h\mu 1}(y, \rho)\psi_{h\mu 1}(y', \rho)\,d\rho + \int_0^{v} z_{01}(\sigma)\psi_{h1}(y, \sigma)\psi_{h1}(y', \sigma)\,d\sigma\Big]. \tag{2}$$

$Z_1(y, y')$ is the Green's impedance function of the semi-infinite slab 1. $\psi_{h1}(y)$ is the modal field of the surface wave with characteristic impedance z_{01}; $\psi_{he1}(y, \rho)$ and $\psi_{ho1}(y, \rho)$ represent the even and odd air modes with characteristic impedance $z_{01}(\rho)$ and $\psi_{h1}(y, \sigma)$ the substrate mode with characteristic impedance $z_{01}(\sigma)$.

Similarly at $x = L^+$, we have

$$E(L, y) = \int_{-\infty}^{\infty} Z_3(y, y')[-H(L, y')]\, dy' \equiv \hat{Z}_3[-H(L, y')] \tag{3}$$

where

$$Z_3(y, y') = z_{03}\psi_{h3}(y)\psi_{h3}(y') + \sum_{\mu=e,o}\int_0^{\infty} z_{03}(\rho)\psi_{h\mu 3}(y, \rho)\psi_{h\mu 3}(y', \rho)\, d\rho + \int_0^{v} z_{03}(\sigma)\psi_{h3}(y, \sigma)\psi_{h3}(y', \sigma)\, d\sigma. \tag{4}$$

$Z_3(y, y')$ is the Green's impedance function of the semi-infinite slab 3. $\psi_{h3}(y)$ is the modal field of the surface wave with characteristic impedance z_{03}; $\psi_{he3}(y, \rho)$ and $\psi_{ho3}(y, \rho)$ represent the even and odd air modes with characteristic impedance $z_{03}(\rho)$ and $\psi_{h3}(y, \sigma)$ the substrate mode with characteristic impedance $z_{03}(\sigma)$. The characteristic impedance for air and substrate mode for slab 1 and 3 are the same given by

$$z_{01}(\rho) = z_{03}(\rho) = z_0(\rho)$$
$$z_{01}(\sigma) = z_{03}(\sigma) = z_0(\sigma).$$

$\hat{Z}_1$ and $\hat{Z}_3$ can be viewed as the driving-point impedance operators of the semi-infinite slabs 1 and 3. In order to relate the total fields at $x = 0$ and $x = L$ in the region 2, a magnetic wall is placed at $x = 0$ and $x = L$ in turn and the relationship between the transverse E and transverse H field for each condition is derived. With a magnetic wall at $x = L$, the transverse electric field $E(0, y)$ excited by magnetic field $H(0, y)$ is given by

$$E(0, y) = \int_{-\infty}^{\infty} Z_{11}(y, y')[-H(0, y')]\, dy' \equiv \hat{Z}_{11}[-H(0, y')] \tag{5}$$

where

$$Z_{11}(y, y') = z_{02}\coth(\gamma_{sh2}L)\phi_{h2}(y)\phi_{h2}(y') + \sum_{\mu=e,o}\int_0^{\infty} z_0(\rho)\coth(\gamma_h L)\cdot\phi_{h\mu 2}(y, \rho)\phi_{h\mu 2}(y', \rho)\, d\rho + \int_0^{v} z_0(\sigma)\coth(\eta_h L)\phi_{h2}(y, \sigma)\cdot\phi_{h2}(y', \sigma)\, d\sigma. \tag{6}$$

Moreover, under the same boundary conditions, we have

$$E(L, y) = \int_{-\infty}^{\infty} Z_{21}(y, y')[-H(0, y')]\, dy' \equiv \hat{Z}_{21}[-H(0, y')] \tag{7}$$

where

$$Z_{21}(y, y') = z_{02}\,\mathrm{cosech}(\gamma_{sh2}L)\phi_{h2}(y)\phi_{h2}(y') + \sum_{\mu=e,o}\int_0^{\infty} z_0(\rho)\,\mathrm{cosech}(\gamma_h L)\cdot\phi_{h\mu 2}(y, \rho)\phi_{h\mu 2}(y', \rho)\, d\rho + \int_0^{v} z_0(\sigma)\,\mathrm{cosech}(\eta_h L)\phi_{h2}(y, \sigma)\cdot\phi_{h2}(y', \sigma)\, d\sigma. \tag{8}$$

When a magnetic wall is placed at $x = 0$, we have by symmetry:

$$E(L, y) \equiv \hat{Z}_{22}[-H(L, y')] \tag{9}$$

and

$$E(0, y) \equiv \hat{Z}_{12}[-H(L, y')] \tag{10}$$

where $\hat{Z}_{22} = -\hat{Z}_{11}$ and $\hat{Z}_{12} = -\hat{Z}_{21}$.

Combining (5), (7), (9), and (10) we obtain a "two port" Green's open circuit impedance operator for the section $0 \le x \le L$ given by

$$\begin{bmatrix} E(0, y) \\ E(L, y) \end{bmatrix} = \begin{bmatrix} \hat{Z}_{11} & -\hat{Z}_{21} \\ \hat{Z}_{21} & -\hat{Z}_{11} \end{bmatrix} \begin{bmatrix} -H(0, y) \\ -H(L, y) \end{bmatrix}. \tag{11}$$

In (2), (4), (6), and (8) we have implicitly assumed that just one surface wave (in y) may be supported by the slab waveguides, and the various value of characteristic impedances are given by

$$z_{01} = \frac{j\omega\mu_0\gamma_{sh1}}{\beta^2 - \gamma_{sh1}^2}; \quad z_{03} = \frac{j\omega\mu_0\gamma_{sh3}}{\beta^2 - \gamma_{sh3}^2};$$
$$z_{02} = \frac{j\omega\mu_0\gamma_{sh2}}{\beta^2 - \gamma_{sh2}^2}$$
$$z_0(\rho) = \frac{j\omega\mu_0\gamma_h}{k_0^2 - \rho^2}; \quad z_0(\sigma) = \frac{j\omega\mu_0\eta_h}{\epsilon_2 k_0^2 - \sigma^2}$$
$$\epsilon_{eh1}k_0^2 - \beta^2 = -\gamma_{sh1}^2; \quad \epsilon_{eh2}k_0^2 - \beta^2 = -\gamma_{sh2}^2;$$
$$\epsilon_{eh3}k_0^2 - \beta^2 = -\gamma_{sh3}^2$$
$$k_0^2 - \beta^2 - \rho^2 = -\gamma_h^2; \quad \epsilon_2 k_0^2 - \beta^2 - \sigma^2 = -\eta_h^2;$$
$$v = k_0\sqrt{\epsilon_2 - \epsilon_3}$$

where ϵ_{eh1}, ϵ_{eh2}, ϵ_{eh3} are the effective dielectric constants (TE polarization) of the slabs 1, 2, and 3, respectively.

Having obtained the two port impedance operators for each uniform section of the waveguide as given by (11), we are now in a position to consider the cascade of steps

in Fig. 1. From (11) the relationship between the transverse fields at x_i and x_{i+1} can be written as

$$\begin{bmatrix} E(x_i, y) \\ E(x_{i+1}, y) \end{bmatrix} = \begin{bmatrix} \hat{Z}_{11}^{(i)} & -\hat{Z}_{21}^{(i)} \\ \hat{Z}_{21}^{(i)} & -\hat{Z}_{11}^{(i)} \end{bmatrix} \begin{bmatrix} -H(x_i, y) \\ -H(x_{i+1}, y) \end{bmatrix}. \quad (12)$$

If the continuity of the transverse fields is translated in to the continuity of voltages and currents at the interface plane x_i and the interface field is approximated by a scalar function, then the cascade of steps in Fig. 1 can be represented by an equivalent "T" network shown in Fig. 2(a). In this formulation the interaction via the propagating air and substrate modes between non adjacent discontinuities is built in to the model, as $E(x_i, y)$ in (12) represents the total transverse field at x_i. If we disregard interaction via propagating continuum modes, then the equivalent network reduce to that of Fig. 2(c). The application of this theory to the analysis of coupled and multiple coupled guides will be treated in Section III.

LSM Analysis

By placing an electric wall at $x = 0$ and $x = L$ in Fig. 3, and by development analogous to that of LSE case we obtain a "two-port" Green's short circuit admittance operator for the length of the waveguide $0 \le x \le L$ given by

$$\begin{bmatrix} -H(0, y) \\ -H(L, y) \end{bmatrix} = \begin{bmatrix} \hat{Y}_{11} & \hat{Y}_{12} \\ \hat{Y}_{21} & \hat{Y}_{22} \end{bmatrix} \begin{bmatrix} E(0, y) \\ E(L, y) \end{bmatrix} \quad (13)$$

where, $\hat{Y}_{12} = -\hat{Y}_{21}$ and $\hat{Y}_{22} = -\hat{Y}_{11}$.

The various quantities occurring in (13) are dual to those occurring in (11) with

$$\begin{aligned} Y_{11}(y, y') &= y_{02} \coth(\gamma_{se2} L)\phi_{e2}(y)\phi_{e2}(y') \\ &\quad + \sum_{\mu = e,o} \int_0^\infty y_0(\rho) \coth(\gamma_e L) \\ &\quad \cdot \phi_{e\mu 2}(y, \rho)\phi_{e\mu 2}(y', \rho)\, d\rho \\ &\quad + \int_0^v y_0(\sigma) \coth(\eta_e L)\phi_{e2}(y, \sigma) \\ &\quad \cdot \phi_{e2}(y', \sigma)\, d\sigma \end{aligned} \quad (14)$$

and

$$\begin{aligned} Y_{21}(y, y') &= y_{02} \operatorname{cosech}(\gamma_{se2} L)\phi_{e2}(y)\phi_{e2}(y') \\ &\quad + \sum_{\mu = e,o} \int_0^\infty y_0(\rho) \operatorname{cosech}(\gamma_e L) \\ &\quad \cdot \phi_{e\mu 2}(y, \rho)\phi_{e\mu 2}(y', \rho)\, d\rho \\ &\quad + \int_0^v y_0(\sigma) \operatorname{cosech}(\eta_e L)\phi_{e2}(y, \sigma) \\ &\quad \cdot \phi_{e2}(y', \sigma)\, d\sigma. \end{aligned} \quad (15)$$

The driving point admittance operator of slab 1, 3 is given by

$$\begin{aligned} Y_1(y, y') &= y_{01}\psi_{e1}(y)\psi_{e1}(y') \\ &\quad + \sum_{\mu = e,o} \int_0^\infty y_0(\rho)\psi_{e\mu 1}(y, \rho)\psi_{e\mu 1}(y', \rho)\, d\rho \\ &\quad + \int_0^v y_0(\sigma)\psi_{e1}(y, \sigma)\psi_{e1}(y', \sigma)\, d\sigma \end{aligned} \quad (16)$$

and

$$\begin{aligned} Y_3(y, y') &= y_{03}\psi_{e3}(y)\psi_{e3}(y') \\ &\quad + \sum_{\mu = e,o} \int_0^\infty y_0(\rho)\psi_{e\mu 3}(y, \rho)\psi_{e\mu 3}(y', \rho)\, d\rho \\ &\quad + \int_0^v y_0(\sigma)\psi_{e3}(y, \sigma)\psi_{e3}(y', \sigma)\, d\sigma. \end{aligned} \quad (17)$$

In (14) to (17) the wavenumbers and modal functions are those appropriate to the TM case. The various admittance occurring in (14) to (17) are given by

$$y_{01} = \frac{j\omega\epsilon_0\gamma_{se1}}{\beta^2 - \gamma_{se1}^2}; \quad y_{03} = \frac{j\omega\epsilon_0\gamma_{se3}}{\beta^2 - \gamma_{se3}^2}; \quad y_{02} = \frac{j\omega\epsilon_0\gamma_{se2}}{\beta^2 - \gamma_{se2}^2}$$

$$y_0(\rho) = \frac{j\omega\epsilon_0\gamma_e}{k_0^2 - \rho^2}; \quad y_0(\sigma) = \frac{j\omega\epsilon_0\eta_e}{\epsilon_2 k_0^2 - \sigma^2}$$

and the wavenumbers are given by

$$\epsilon_{ee1}k_0^2 - \beta^2 = -\gamma_{se1}^2; \quad \epsilon_{ee2}k_0^2 - \beta^2 = -\gamma_{se2}^2;$$

$$\epsilon_{ee3}k_0^2 - \beta^2 = -\gamma_{se3}^2$$

$$k_0^2 - \beta^2 - \rho^2 = -\gamma_e^2; \quad \epsilon_2 k_0^2 - \beta^2 - \sigma^2 = -\eta_e^2;$$

$$v = k_0\sqrt{\epsilon_2 - \epsilon_3}$$

where ϵ_{ee1}, ϵ_{ee2}, ϵ_{ee3} are the effective dielectric constants (TM polarization) of the slabs 1, 2, and 3, respectively.

Using (13) and translating the continuity of the transverse fields at each port in to the continuity of voltages and currents and approximating the interface field by a scalar function we recover the equivalent network for the cascade of steps as shown in Fig. 2(b). The application of the theory to the analysis of coupled structures will be discussed in Section III.

III. Numerical Solution of Coupled Rib Waveguides

Directional Couplers

The cross sectional geometry of a straight rib waveguide directional coupler is shown in Fig. 4(a). The two guides are identical. The field distribution of this structure shown in Fig. 4(b) comprises the even and odd modes propagating along the coupler with propagation constants β_e and β_o, respectively. Including time and z-dependence the even and odd mode amplitudes may be expressed as

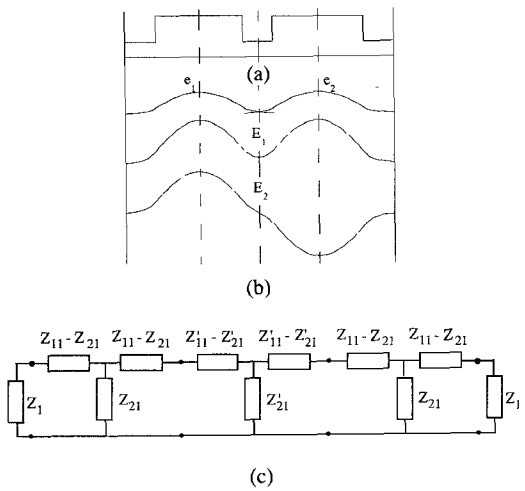

Fig. 4. (a) Cross sectional geometry of straight rib waveguides directional coupler; (b) The even (E_1) and odd (E_2) field distribution of the structure; (c) Equivalent network modeling of the directional coupler.

$$\text{for the even mode } E(z) \approx \cos(\omega t - \beta_e z)$$

$$\text{for the odd mode } E(z) \approx \cos(\omega t - \beta_o z).$$

By linearity the response of the structure is given by the superposition of the even and odd mode responses. If the even and odd modes are excited with equal amplitudes we have, for guide 1,

$$\begin{aligned} E_1(z) &= A\cos(\omega t - \beta_e z) + A\cos(\omega t - \beta_o z) \\ &= 2A\cos\left(\omega t - \frac{\beta_e + \beta_o}{2} z\right)\cos\left(\frac{\beta_e - \beta_o}{2} z\right) \\ &= 2A\cos(\omega t - \beta z)\cos(cz) \end{aligned}$$

for guide 2,

$$\begin{aligned} E_2(z) &= A\cos(\omega t - \beta_e z) - A\cos(\omega t - \beta_o z) \\ &= 2A\sin\left(\omega t - \frac{\beta_e + \beta_o}{2} z\right)\sin\left(-\frac{\beta_e - \beta_o}{2} z\right) \\ &= 2A\sin(\omega t - \beta z)\sin(-cz). \end{aligned}$$

Along the length of the coupler L_t, the relative phases of the two modes will reverse and at this point the mode fields reinforce each other in the opposite sense, accounting for the transfer of power between the two guides of the coupler. For this to occur,

$$\cos\left(\frac{\beta_e - \beta_o}{2} L_t\right) = 0$$

$$\frac{\beta_e - \beta_o}{2} L_t = \frac{n\pi}{2}; \qquad n \text{ odd}$$

$$L_t = \frac{n\pi}{\beta_e - \beta_o} \tag{18}$$

where L_t is the transfer length for maximum power transfer.

If even and odd modes are not excited with equal amplitudes, then, when the two modes are out of phase, cancellation in one of the guides will not be complete. Hence, a small amount of power will be left which may contribute to the crosstalk. In this work emphasis is given to the determination of transfer lengths, a useful parameter required to characterize the coupler and the problems of crosstalk are not pursued further. Most practical structures are considered to be strongly coupled. For example, short transfer lengths are desired for small and fast switches. The key to evaluating the transfer length of a coupler is the calculation of β_e and β_o. Hence, an appropriate technique accurate for strongly coupled situation is highly desirable to determine the propagation constants. This is done using the theory developed in the previous section. The equivalent network modeling of the structure is shown in Fig. 4(c). In this case, solving the coupled structure reduces to that of solving the equivalent network. This is achieved more effectively by cascade multiplication of the transfer matrices of the individual networks. The transfer matrix relates voltages and currents at the LHS ports to the RHS is given by

$$T = \begin{bmatrix} \hat{Z}_{11}\hat{Z}_{21}^{-1} & -\hat{Z}_{11}\hat{Z}_{22}\hat{Z}_{21}^{-1} + \hat{Z}_{12} \\ \hat{Z}_{21}^{-1} & -\hat{Z}_{21}^{-1}\hat{Z}_{22} \end{bmatrix}$$

The z-directed propagation constants β_e and β_o of the even and odd modes respectively are determined from the transverse resonances condition applied at a chosen reference point. By using simple network theory and choosing reference point at $x = 0$, we obtained the scalar dispersion equation given by

$$\hat{Z}_1 + \hat{Z}_{IN} = 0; \quad \text{for LSE polarization}$$

$$\hat{Y}_1 + \hat{Y}_{IN} = 0; \quad \text{for LSM polarization}$$

where $\hat{Z}_{IN}$ and $\hat{Y}_{IN}$ is the input impedance and admittance respectively looking to the right of $x = 0$. Solving the dispersion equation yields the propagation constants β_e and β_o.

In order to demonstrate the accuracy of the present technique we consider first the directional couplers analyzed by [8] using the Finite Difference Method. The parameters describing the directional couplers analyzed in [8] are given in Table I. The results of the present analysis together with those of FDM and the EDC method are summarized in Table II. Simulations indicate that both present and FDM analysis results agree very well and prove the accuracy of the present method. The results of the EDC agree very well with the present and FDM analysis only for small rib height. As shown in Table II, the present method does not produce the odd mode index for the third structure. This is because the odd mode for this structure is cutoff and the mode index is complex. This argument is justified by examining the index of the odd mode predicted by FDM analysis β_o/k_0 is less than the EDC of the outer slab $\sqrt{\epsilon'_{eh}}$. The computer program used in the present analysis is developed to predict real mode index β_o/k_0 in the range $\sqrt{\epsilon'_{eh}} < \beta_{e,o}/k_0 < \sqrt{\epsilon_{eh}}$.

TABLE I
PARAMETERS OF THE DIRECTIONAL COUPLER WHICH HAVE BEEN ANALYZED

Rib Guide Structure	n_1	n_2	n_3	D μm	d μm	L μm	S μm	λ μm
1	3.44	3.34	1.0	1.3	0.2	2.0	2.0	1.55
2	3.44	3.36	1.0	1.0	0.9	3.0	2.0	1.55
3	3.44	3.435	1.0	6.0	3.5	4.0	2.0	1.55

TABLE II
MODAL REFRACTIVE INDICES OF EVEN AND ODD MODES IN DIRECTIONAL COUPLER STRUCTURES

Structure	Mode Indices	TRD Using Fig. 2(a)	TRD Using Fig. 2(c)	FDM [8]	EDC
ST1	β_e/k_0	3.388841027	3.388838939	3.391472377	3.390322424
	β_o/k_0	3.388841027	3.388838350	3.391470106	3.390322421
	L_t [mm]	—	1314.57	341.0	300000.0
ST2	β_e/k_0	3.395739365	3.395739353	3.396053426	3.395914969
	β_o/k_0	3.394802846	3.394802837	3.395097562	3.394954357
	L_t [mm]	0.827	0.827	0.811	0.807
ST3	β_e/k_0	3.436820329	3.436806957	3 437034755	3.437661171
	β_o/k_0	—	—	3.436459357	3.437072754
	L_t [mm]	—	—	1.347	1.317

This is not a limitation of the method and if complex algebra is used in the computer program it should be able to yield a complex index for this mode. However, this problem is not pursued further as emphasis in this work is focussed on the determination of transfer length of coupled guides. In order to assess the effect of the propagating continuous modes on the transfer length of coupled guides at optical frequencies, we compare the results of the analysis using equivalent networks in Fig. 2(a) and Fig. 2(c). The parameters of the structure examined in this exercise are $n_1 = 3.44$, $n_2 = 3.40$, $n_3 = 1.0$, $D = 1$ μm, $L = 3$ μm, $\lambda = 1.15$ μm, $S = 2$ μm and d varying. The results of the simulations are summarized in Table III. Simulations indicate that the effect of the propagating continuous modes on the transfer length is small even for well confined modes. This observation shows that at optical frequencies with $n_1 >> n_3$, the interaction via the continuous modes is small and can be neglected. Hence, it is possible to obtain accurate results by considering interaction via the surface modes only and using the simpler equivalent network Fig. 2(c).

Having established the accuracy of the technique, we are in a position to consider some numerical results that can be utilized as design data. The parameters of the coupled structure considered are shown in the figure. The variation of the modal indices of the even and odd modes as a function of the guide separation S is shown in Fig. 5. The even and odd mode indices are above and below the single guide index, respectively. For small guides separation S, i.e., for strongly coupled system, the differences of even and odd modes indices from the single guide index are not equal and hence $\beta \neq (\beta_e + \beta_o)/2$.

TABLE III
COMPARISON OF MODAL REFRACTIVE INDICES OF EVEN AND ODD MODES AND TRANSFER LENGTH OF DIRECTIONAL COUPLER STRUCTURE FOR DIFFERENT OUTER SLAB HEIGHT

d μm	Mode Indices	Using Model Fig. 2(a)	Using Model Fig. 2(c)	Difference %
0.3	β_e/k_0	3.412597677	3.412595607	
	β_o/k_0	3.412551746	3.412549877	
	L_t [mm]	12.5272	12.5739	0.37
0.6	β_e/k_0	3.413685884	3.413685555	
	β_o/k_0	3.413535726	3.413535438	
	L_t [mm]	3.831		0.025
0.9	β_e/k_0	3.415891467	3.415891456	
	β_o/k_0	3.415203392	3.415203383	
	L_t [mm]	0.835666	0.835666	0

As the guide separation S increases both β_e/k_0 and β_o/k_0 appear to approach the single guide index and for sufficiently large S they become almost equally spaced from β/k_0. This behavior is consistent with the prediction of coupled mode theory and β can be accurately predicted by $\beta = (\beta_e + \beta_o)/2$. This occurs when the coupling is loose. This observation shows that, for a strongly coupled system, coupled mode theory is less than accurate and more rigorous analyses such as the present method should be used. The transfer lengths can be calculated using the data in Fig. 5 and the plot of L_t versus S is shown in Fig. 6. The transfer length increases exponentially with increasing S. This shows that coupling decreases exponentially as S is increased. This behavior is direct consequence of the fact that fields decay exponentially outside

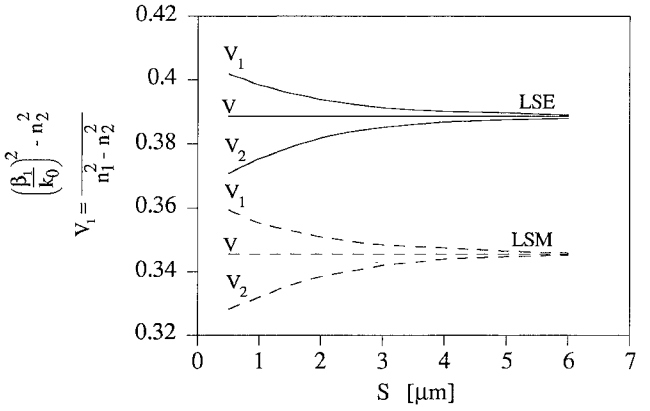

Fig. 5. Variation of the normalized modal indices of the even and odd modes as a function of the guide separation S for directional coupler. V_1-even mode, V_2-odd mode, V-mode of single guide. The values of the parameters of the directional coupler ST4 are: $n_1 = 3.44$, $n_2 = 3.40$, $n_3 = 1.0$, $D = 1$ μm, $d = 0.9$ μm, $L = 3.0$ μm, $\lambda = 1.15$ μm.

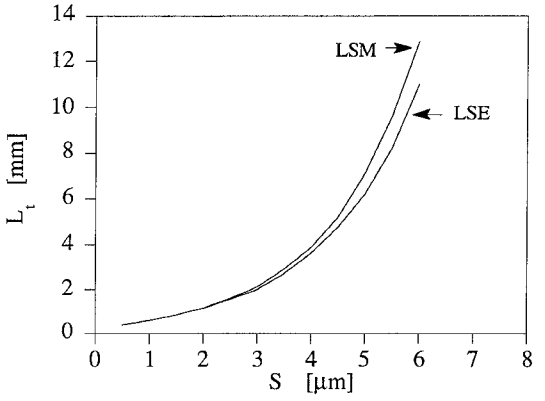

Fig. 6. Variation of the transfer length L_t as a function of guides separation S for directional coupler ST4.

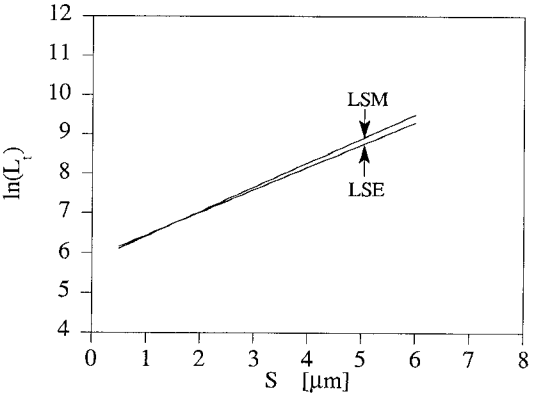

Fig. 7. Variation of $ln(L_t)$ as a function of guides separation S for directional coupler ST4.

the guides. Their decay constant may be predicted from the gradient of the plot of $ln(L_t)$ versus S given in Fig. 7.

Three Guide-Couplers

A symmetrical three guide-coupler composed of three identical rib waveguides in close proximity is shown in Fig. 8(a). The individual waveguides are assumed to be

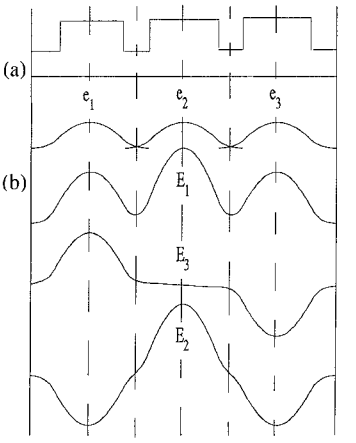

Fig. 8. (a) Cross sectional geometry of three identical rib waveguide coupler; (b) The transverse field profiles of the overlapping guides modes and the modes of the coupled structure.

single moded. Before applying the present method of analysis, it is instructive to consider the modal characteristics of this structure. The transverse field profiles of the overlapping guides modes and the modes of the coupled structure in Fig. 8(a) are shown in Fig. 8(b). The coupled structure has three modes, two are even with propagation constants β_1 and β_2 and one is odd with propagation constant β_3. In [11], a similar configuration has been analyzed using the EDC technique and it has been shown that the propagation constants of the three modes obey the following conditions:

$$\beta_1 > \beta$$

$$\beta_2 > \beta$$

$$\beta_3 \lesseqgtr \beta; \quad \text{depending on the guide parameters}$$

$$(\beta_3 - \beta) \leq (\beta_1 - \beta) \quad \text{or} \quad (\beta_2 - \beta) \tag{19}$$

where β is the modal propagation constant of a single isolated rib waveguide.

There are two possible ways to excite the structure in Fig. 8(a). In the first case, the structure is excited symmetrically through the center guide and this configuration may be used as a power divider. In this case only modes 1 and 2 are excited, such that at $z = 0$ their fields are in phase i.e., additive in the center guide and subtractive in the outside guides. At some distance z down the line, modes 1 and 2 get out of phase, their fields interfere destructively in the center guide and constructively in the outside guides, accounting for the transfer of power from the center guide to the outside guides. This occurs at multiples of the coupling length given by [11],

$$L_{ct} = \frac{\pi}{\beta_1 - \beta_2}. \tag{20}$$

In the second case, the three guide coupler is excited antisymmetrically through either one of the outer guides. Such configuration may be used to transfer power from one of the outer guides to the other outer guide. The fea-

sibility of using such device as an improved sampler has been demonstrated in [12]. At $z = 0$, modes 1 and 2 are excited out of phase so that they are in antiphase in the centre guide and in phase in the outer guides. Mode 3 is excited so it is in phase with modes 1 and 2 in the input outer guide and antiphase in the other outer guide. In this case, the situation is more complex and beats periodic with distance down the coupler can only be obtained with high power transfer efficiency between guides if the phase velocities of the modes are related to each other in a simple manner. Under the condition of loose coupling most of the power will be transferred from one outer guide to the other at a length given by [11]

$$L_{ot} = \frac{2\pi}{\beta_1 - \beta_2}; \tag{21}$$

i.e., the coupling length is twice that required to symmetrically transfer power from the center guide to the two outer guides.

Again the key parameter in the analysis of the three guide coupler is the accurate evaluation of β_1, β_2, and β_3. In this numerical example, three guides of the geometry used in the previous example will be analyzed. The resulting equivalent circuit is similar to that of Fig. 4(c) but includes two additional network sections corresponding to the third guide. Solving the equivalent circuit yields all the β's values. Equation (19) is used as a reference in the identification of β values for the two even modes and odd mode. The variation of the effective indices of the even modes and odd mode as a function of separation between the guides S are shown in Fig. 9. The straight line is the effective index of the single isolated rib waveguide. Using Fig. 9 the length required to transfer power from the center guide to the outer guides, L_{ct}, can be calculated using (20) and that to transfer power from one of the outer guides to the other, L_{ot}, can be obtained from (21). The variation of $ln(L_{ct})$ and $ln(L_{ot})$ as a function of guides separation S is plotted in Fig. 10. In Fig. 11 the variation of the transfer length of the three guide coupler and of the directional coupler is shown as a function of guides separation S. Comparing the two curves, it can be seen that for strongly coupled structures the ratio of the two transfer lengths is between 1.45 and 1.5.

Only for loosely coupled structures does the ratio become very close to $\sqrt{2}$, i.e., the prediction of coupled mode theory. There are two points to be noted from this observation. Firstly, accurate analyses should be employed even for most practical devices. Secondly, one must beware when using data derived from two guide couplers to design devices with three guide couplers. In fact, a simple $\sqrt{2}$ relationship between the transfer lengths predicted by coupled mode theory does not hold for strongly coupled situations.

Strongly Coupled Unequal Guides

The theory developed in Section II applies not only to structures with identical rib waveguides but also to structures with rib guides of different dimensions. As an example, we investigate the propagation constants of strongly coupled unequal guides where the geometrical dimensions of guide 1 are fixed and the rib width or rib height of guide 2 varies. The other dimensions of guide 2 are fixed. The optical parameters of the guides are n_1 =

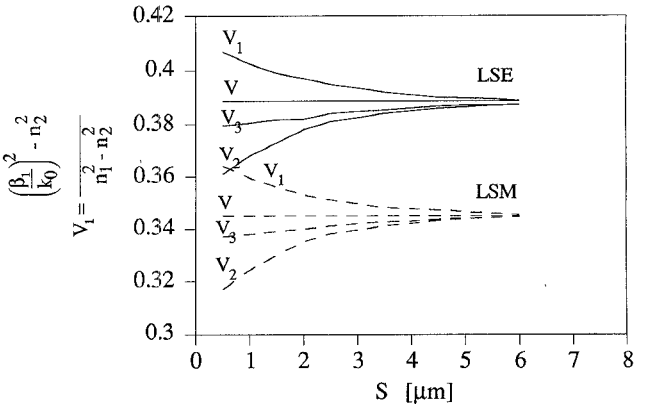

Fig. 9. Variation of the normalized modal indices of the even and odd modes as a function of guides separation S for three guide coupler. V_1, V_2-even modes, V_3-odd mode, V-mode of single guide. The values of the parameters of the three guide coupler ST5 are: $n_1 = 3.44$, $n_2 = 3.40$, $n_3 = 1.0$, $D = 1$ μm, $d = 0.9$ μm, $L = 3.0$ μm, $\lambda = 1.15$ μm.

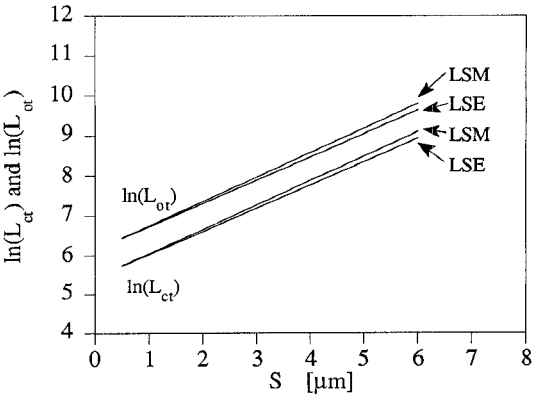

Fig. 10. Variation of $ln(L_{ct})$ and $ln(L_{ot})$, as a function of guides separation S for three guide coupler ST5.

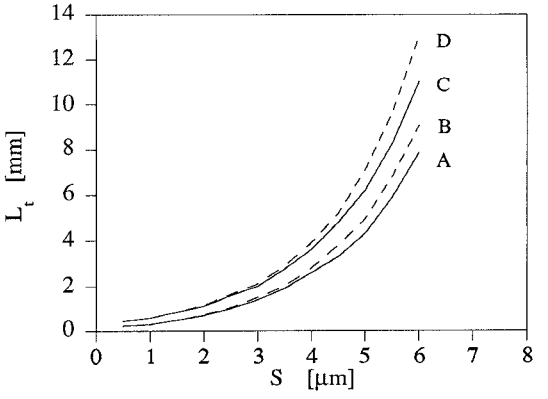

Fig. 11. Variation of the transfer length of the three guide coupler ST5 L_{ct} (Curves A and B) and of the directional coupler ST4 L_t, (curves C and D) as a function of guides separation S. Continuous lines refer to LSE analysis; dashed lines refer to LSM analysis.

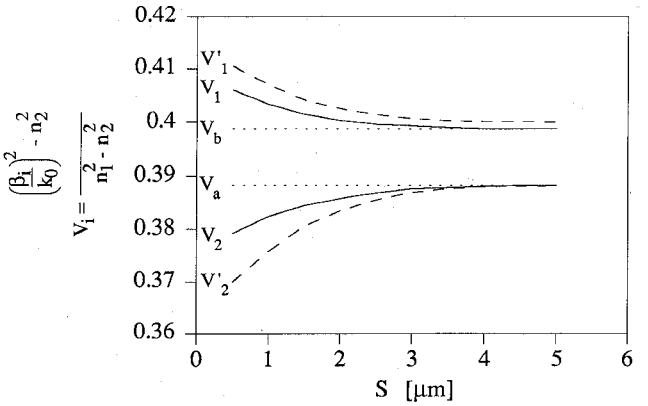

Fig. 12. Variation of the normalized modal indices (LSE) of the modes as a function of guide spacing for closely coupled nonidentical guide. Curve V_a and V_b are V's for uncoupled guide of $L = 3.0$ μm and 4.0 μm, respectively and $D = D' = 1.0$ μm, $d = 0.9$ μm. Continuous line (V_1, V_2): $L = 3.0$ μm, $L' = 4.0$ μm, $d = 0.9$ μm, $D = 1.0$ μm, $D' = 1.0$ μm. Dashed line (V_1', V_2'): $L = 3.0$ μm, $L' = 4.0$ μm, $d = 0.9$ μm, $D = 1.0$ μm, $D' = 1.2$ μm.

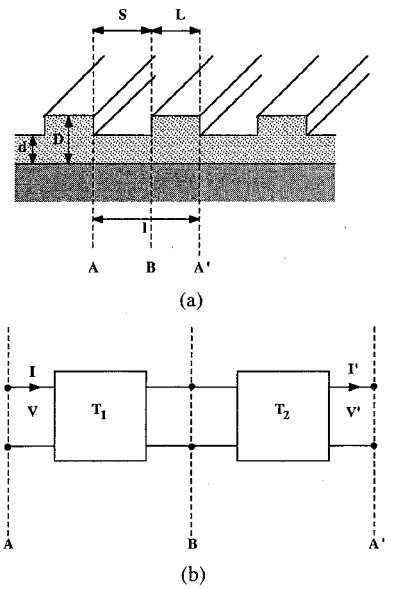

Fig. 13. (a) Rib waveguide arrays: (b) Equivalent circuit representation for the unit element of the periodic structure.

3.44, $n_2 = 3.40$, $n_3 = 1.0$, and $\lambda = 1.15$ μm. Their geometrical dimensions are reported in the figure. The results for the modal indices as a function of the guide separation are shown in Fig. 12. From the figure, it can be seen that the fundamental modes of the two rib waveguides are not synchronous where each of the two modes favors one of the two rib waveguides. Thus, each mode is nearly equal to the mode of one or the other rib waveguide taken in isolation. For sufficiently large guides separation the two guides decoupled. These two fundamental modes would have even and odd symmetry if both rib waveguides were identical. From this observation it can be seen that in order to achieve a nonidentical guides coupler the two guides ought to be strongly coupled and in synchronism so that the two modes can be superimposed such that at the input end of the coupler their fields nearly cancel in one guide while they reinforce each other in the opposite guide. At a distance $L_t = \pi/(\beta_2 - \beta_1)$ the mode fields reinforce each other in opposite sense, accounting for the transfer of power between the two guides. In order to achieve synchronism of the two guides the rib width or the rib height may be adjusted.

Waveguide Arrays

An array of coupled rib waveguides is shown in Fig. 13. This configuration has been used to design coupled laser arrays [13]. The operation of coupled waveguide arrays is more complicated than that of a two or three-guide coupler because of the higher number of modes which can exist in the structures. If the individual guides are single moded, then the number of possible guided modes of coupled arrays is generally equal to the number of guides in the array [10]. The propagation constants of the structure can be obtained by using the theory developed in Section II. In the case of finite arrays, the numerical evaluation of the propagation constants is similar to that of a three guide coupler with little additional computation. The increase in computation time is small since we are dealing with only an additional multiplication of the transfer matrices and there is no need to calculate an additional equivalent circuit parameters.

If the array is large and periodic we may approximate its propagation constant, in a manner similar to the determination of the propagation constant of a cascaded transmission line. To solve a periodic structure let consider the unit element of the periodic structure and its equivalent circuit shown in Fig. 13. The relationship between voltages and currents at A and A' is given by

$$\begin{bmatrix} V \\ I \end{bmatrix} = T_1 \cdot T_2 \begin{bmatrix} V' \\ I' \end{bmatrix} \tag{22}$$

where T is the transfer matrix for each uniform section, already derived in Sections II and III.

The periodicity condition requires

$$\begin{bmatrix} V' \\ I' \end{bmatrix} = e^{-jK_x l} \begin{bmatrix} V \\ I \end{bmatrix} \tag{23}$$

where l is the length of the period and K_x is the propagation constant of the periodic structure. Substituting (23) in to (22) gives the approximate eigenvalue equation for the periodic structure, that is

$$T_1^{-1} \cdot T_2^{-1} \begin{bmatrix} V \\ I \end{bmatrix} = e^{-jK_x l} \begin{bmatrix} V \\ I \end{bmatrix}. \tag{24}$$

IV. Conclusion

In this contribution we develop a simple and effective rigorous solution for coupled rib waveguides. The problem is seen as that of cascaded step discontinuities in the transverse direction. The use of a "transition function" at the discontinuities interface not only simplifies the cal-

culation, avoiding the use of matrices but it also yields a simple cascaded two port network representation of the coupled structure.

The accurate determination of the propagation constants of the modes of the coupled structure is very important in determining the coupling between waveguides. The method developed in this work is believed to be accurate and is valid under all circumstances of both strong and weak coupling. The accuracy of the method was demonstrated by comparing the results with the results of FDM calculations. Numerical examples were carried out and, where comparison is available, it has been found the method yields results that compare very favorably with those produced by FDM. Numerical simulations also show that the results of coupled mode theory agree with our accurate results only for weakly coupled structures. As most practical devices are in fact tightly coupled, more accurate analyses such as the present method, should be employed in their study. The additional computational effort required to analyze multiple guide couplers including arrays and non-identical guides using the present method is only marginally higher than that required for a single guide. This is the important advantage of this method over numerical methods where the computational effort increases as the area of the cross section increases.

REFERENCES

[1] U. Crombach, "Analysis of single and coupled rectangular dielectric waveguides," *IEEE Trans. Microwave Theory Tech.*, vol. MTT-29, no. 9, pp. 870–874, Sept. 1981.

[2] M. R. Knox and P. P. Toulios, "Integrated circuits for the millimeter through optical frequency range," in *Proc. of Symp. on Submillimeter Waves*, Polytechnic Institute of New York, 1970, pp. 497–516.

[3] W. V. McLevige, T. Itoh, and R. Mittra, "New waveguide structure for millimeter wave and optical integrated circuits," *IEEE Trans. Microwave Theory Tech.*, vol. MTT-23, no. 10, pp. 788–794, Oct. 1975.

[4] T. Trinh and R. Mittra, "Coupling characteristics of planar dielectric waveguides of rectangular cross section," *IEEE Trans. Microwave Theory Tech.*, vol. MTT-29, no. 9, pp. 875–880, Sept. 1981.

[5] A. Yariv, "Coupled mode theory for guided wave optics," *IEEE J. Quantum Electron.*, vol. QE-9, p. 919, 1973.

[6] A. Hardy and W. Streifer, "Coupled mode solutions of multiwaveguide systems," *IEEE J. Quantum Electron.*, vol. QE-22, pp. 528–534, Apr. 1986.

[7] H. A. Haus, W. P. Huang, S. Kawakami, and N. A. Whitaker, "Coupled mode theory of optical waveguides," *J. Lightwave Technol.*, vol. LT-5, no. 1, pp. 16–23, Jan. 1987.

[8] M. J. Robertson, S. Ritchie, and P. Dayan, "Semiconductor waveguides: Analysis of optical propagation in single rib structures and directional couplers," *Proc. Inst. Elec. Eng*, vol. 132, pt. J, no. 6, Dec. 1985.

[9] T. Rozzi, G. Cerri, M. N. Husain, and L. Zappelli, "Variational analysis of the dielectric rib waveguide using the concept of "Transition Function" and including edge singularities," *IEEE Trans. Microwave Theory Tech.*, vol. 39, no. 2, pp. 247–257, Feb. 1991.

[10] T. Rozzi and G. H. In't Veld, "Field and network analysis of interacting step discontinuities in planar dielectric waveguide," *IEEE Trans. Microwave Theory Tech.*, vol. MTT-27, no. 4, pp. 303–309, Apr. 1979.

[11] J. P. Donnely, N. L. De Meo, and G. A. Ferrante, "Three guide couplers in GaAs," *J. Lightwave Technol.*, vol. LT-1, no. 2, pp. 417–424, June 1983.

[12] H. A. Haus and C. G. Fonstad, "Three waveguide couplers for improved sampling and filtering," *IEEE J. Quantum Electron.*, vol. QE-17, pp. 2321–2325, Dec. 1981.

[13] Y. Twu, A. Dienes, S. Wang, and J. R. Whinnery, "High power coupled ridge waveguide semiconductor laser arrays," *Appl. Phys. Lett.*, vol. 45, pp. 709–711, Oct. 1984.

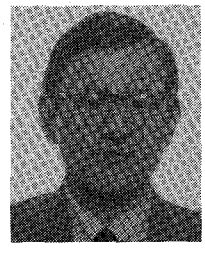

Tullio Rozzi (M'66–SM'74–F'90) obtained the degree of 'Dottore' in physics from the University of Pisa in 1965, and the Ph.D. degree in electronic engineering from Leeds University in 1968. In June 1987 he received the degree of D.Sc. from the University of Bath, Bath, U.K.

From 1968 to 1978 he was a Research Scientist at the Philips Research Laboratories, Eindhoven, the Netherlands, having spent one year, 1975, at the Antenna Laboratory, University of Illinois, Urbana. In 1975 he was awarded the Microwave Prize by the IEEE Microwave Theory and Technique Society. In 1978 he was appointed to the Chair of Electrical Engineering at the University of Liverpool and was subsequently appointed to the Chair of Electronics and Head of the Electronics Group at the University of Bath, in 1981. From 1983 to 1986 he held the additional position of Head of the School of Electrical Engineering at Bath. Since 1988 he has been Professor of Antennas in the Department of Electronics and Control, University of Ancona, Italy, while remaining a Visiting Professor at Bath University.

Dr. Rozzi is a Fellow of the IEE (U.K.).

M. N. Husain, photograph and biography not available at the time of publication.

Leonardo Zappelli was born in Rome in 1962. He received the "Doctor" degree in electronic engineering from the University of Ancona, Italy, in 1987.

Since 1988 he has been with the Department of Electronics and Automatics at the University of Ancona, as a Research Assistant. His area of interest includes integrated optics, microwaves and electromagnetic compatibility.